Published in final edited form as:
Science. 2009 December 4; 326(5958): 1412–1415. doi:10.1126/science.1177662.

Structural Insight Into Nascent Polypeptide Chain-Mediated Translational Stalling

Birgit Seidelt[1,1,†], **C. Axel Innis**[2,†], **Daniel N. Wilson**[1], **Marco Gartmann**[1], **Jean-Paul Armache**[1], **Elizabeth Villa**[3,4,§], **Leonardo G. Trabuco**[3,4], **Thomas Becker**[1], **Thorsten Mielke**[5], **Klaus Schulten**[3,4,6], **Thomas A. Steitz**[2,7,*], and **Roland Beckmann**[1,*]

[1] Gene Center and Center for integrated Protein Science Munich (CiPSM), Department for Chemistry and Biochemistry, University of Munich, Feodor-Lynen-Str. 25, 81377 Munich, Germany

[2] Department of Molecular Biophysics and Biochemistry, Howard Hughes Medical Institute and Yale University, New Haven, CT 06520, USA.

[3] Beckman Institute, University of Illinois at Urbana-Champaign, Urbana, IL, 61801, USA

[4] Center for Biophysics and Computational Biology, University of Illinois at Urbana-Champaign, Urbana, IL, 61801, USA

[5] UltraStrukturNetzwerk, Max Planck Institute for Molecular Genetics, Ihnestr. 73, 14195-Berlin, Germany and Institut für Medizinische Physik und Biophysik, Charité, Ziegelstr. 5-8, 10117 Berlin, Germany

[6] Department of Physics, University of Illinois at Urbana-Champaign, Urbana, IL, 61801, USA

[7] Department of Chemistry, Yale University, New Haven, CT 06520, USA.

Abstract

Expression of the *Escherichia coli* tryptophanase operon depends upon ribosome stalling during translation of the upstream TnaC leader peptide, a process for which interactions between the TnaC nascent chain and the ribosomal exit tunnel are critical. We determined a 5.8 Å resolution cryo-electron microscopy and single particle reconstruction of a ribosome stalled during translation of the *tnaC* leader gene. The nascent chain was extended within the exit tunnel, making contacts with ribosomal components at distinct sites. Upon stalling, two conserved residues within the peptidyltransferase center adopted conformations that preclude binding of release factors. We propose a model whereby interactions within the tunnel are relayed to the peptidyltransferase center to inhibit translation. Moreover, we show that nascent chains adopt distinct conformations within the ribosomal exit tunnel.

In prokaryotes, proteins are synthesized through translation of mRNA by the 70S ribosome, a large ribonucleoprotein complex consisting of a large (50S) and a small (30S) subunit. While most polypeptides are thought to passively transit through the exit tunnel of the 50S subunit during translation, certain nascent chains appear to specifically interact with or adopt a secondary structure within the exit tunnel (1-3). This can in turn modulate the rate of translation (4) and in some cases induce translational stalling to regulate gene expression (5). For instance,

[*] *To whom correspondence should be addressed.* beckmann@lmb.uni-muenchen.de; thomas.steitz@yale.edu.
[†] These authors contributed equally to this work
[§] *Present address:* Department of Structural Biology, Max Planck Institute of Biochemistry, Am Klopferspitz 18, D-82152 Martinsried, Germany

Supporting Online Material www.sciencemag.org Materials and Methods Figs. S1-S9 Movie S1 Table S1 References

stalling during translation of the SecM leader peptide in *Escherichia coli* (6-8) affects the expression of the downstream *secA* gene (9).

In bacteria translational stalling is also used to regulate the expression of the tryptophan-catabolizing enzymes tryptophanase and tryptophan-specific permease, encoded by the *tnaA* and *tnaB genes*, respectively. In the tryptophanase (*tna*) operon of *E.coli,* the *tnaC* regulatory leader gene is located upstream of these two structural genes (10) and the spacer region between the *tnaC* and *tnaA* genes contains several potential Rho-dependent transcription-termination sites. When free tryptophan levels are low in the cell, the TnaC leader peptide is translated and the ribosomes are released from the mRNA, allowing Rho to access and terminate transcription before the RNA polymerase reaches the *tnaA/B* genes. In the presence of free tryptophan, however, the stalled TnaC•70S complex masks the Rho-dependent transcription-termination sites and thus transcription of the downstream *tnaA/B* genes ensues (10). Trp^{12}, Asp^{16} and Pro^{24} of the 24-residue TnaC leader peptide are crucial for stalling (10-12) and the TnaC•$tRNA^{Pro}$ (Pro^{24}) is located within the P site of the ribosome (13), indicating that Asp^{16} and Trp^{12} are retained within the exit tunnel. Moreover, mutations in ribosomal tunnel components alleviate stalling (11), suggesting that interactions between the TnaC nascent chain and the ribosomal tunnel are an essential feature of the stalling mechanism.

To gain structural insight into the mechanism by which the TnaC leader peptide induces translational stalling, cryo-electron microscopy (cryo-EM) and single-particle analysis were used to reconstruct an empty *E. coli* 70S control ribosome (Fig. 1A, B), and an *E. coli* 70S ribosome stalled during translation of the TnaC leader gene by addition of free tryptophan (TnaC•70S complex; Fig. 1C, D and Fig. S1) (14), at 6.6 Å and 5.8 Å (FSC 0.5 criterion) resolution, respectively (Fig. S2 and S3). A comparison with the empty 70S ribosome (Fig. 1A, B) reveals additional density for a peptidyl-tRNA positioned within the P-site of the TnaC•70S complex and for an mRNA spanning the A-, P- and E-sites (Fig. 1C, D, Fig. S4). An atomic model of the complete TnaC•70S complex, including the mRNA and $tRNA^{Pro}$ at the P-site was generated using Molecular Dynamics Flexible Fitting (MDFF) (15) (Fig. S5). Moreover, additional density within the exit tunnel could be attributed to the TnaC nascent chain (Fig. 1C, D). At high contour levels, density remained very robust for the C-terminal half of the nascent chain (Fig. S6), and continuous density could be seen throughout the entirety of the tunnel at lower contour levels (Fig. 1E). Using density as a restraint, an ensemble of molecular models for residues 4-24 of the TnaC peptide was generated using Rapper (16) and MDFF (15) (Fig. 1F, S7 and Movie S1). In agreement with the experimental density, these models featured an extended nascent chain, with root-mean-square fluctuations (RMSFs) for the Cα atoms smaller than 2 Å (Fig. S7, S8 and Movie S1). Since the resolution in our maps is limited to ~6 Å all subsequent analysis was restricted to the Cα atoms of TnaC.

Inspection of the ribosomal exit tunnel revealed that the density for the TnaC nascent chain fuses with the tunnel wall at a multitude of sites (Table S1 and Fig. 2). At the peptidyl transferase center (PTC) of the ribosome, which is the site of peptide bond formation and peptidyl-tRNA hydrolysis (17), additional density connects Pro^{24} of TnaC and U2585 of the 23S rRNA (Fig. 2A), whereas the neighboring U2586, together with U1782, form a connection in the region where Asp^{21} is likely to be located (Fig. 2A). Mutations in the U2585 region have been shown to reduce the maximum level of tnaC induction (18) and the highly conserved Pro^{24} is known to be essential for stalling (12). Very strong density links G2061 and A2062 to the region near residues Arg^{23} and Asp^{21}, respectively, of TnaC (Fig. 2B). Although A2062 has not been analyzed for its effects on TnaC stalling, mutations at this position relieve the translational arrest mediated by another leader peptide, ErmCL (19). Deeper in the tunnel, two connections are visible linking A2058 and A2059 with the nascent chain in the proximity of Asp^{16} and Lys^{18} (Fig. 2C), which may explain the protection of these nucleotides from sparsomycin-enhanced chemical modification seen during tryptophan-induced TnaC-stalling (20). Asp^{16} is

highly conserved within the TnaC leader peptide and Asp16Ala mutations abolish the Trp-dependent inactivation of the PTC (12). Ribosomes with A2058G mutations are slightly more responsive to Trp-induced stalling in a *rrn* Δ6 strain (11), whereas this mutation strongly alleviates secM-mediated translational stalling (6). Strong density that extends out from the TnaC nascent chain at the putative location for Lys^{18} fuses with the ribosomal tunnel where U2609 and A752 are located, whereas the adjacent nucleotide A751 appears to contact TnaC in the vicinity of Phe^{13} (Fig. 2C). Consistently, mutations at U2609 as well as an insertion at A751 have been reported to eliminate the induction by tryptophan (11). The TnaC nascent chain makes two major contacts with the β-hairpin of ribosomal protein L22 (Fig. 2D): One connects Arg^{95} of L22 with the nascent chain near Thr^{9}, whereas the other is found at the tip of the loop, where Lys^{90} and Arg^{92} are located, and fuses with TnaC in the proximity of the highly conserved Trp^{12} residue (Fig. 2D). This latter contact should be important for TnaC-stalling since (i) the spacing between Trp^{12} and Pro^{24} is critical for efficient stalling (10-12) and (ii) mutations of Trp^{12} in TnaC as well as Lys^{90} in L22 also eliminate tryptophan induction (11). Additional evidence for the close proximity of Trp^{12} to the tip of L22 comes from crosslinks between the neighboring Lys^{11} with 23S rRNA nucleotides in the vicinity of A751 (11), which also makes contact with the tip of the β-hairpin of L22 (Fig. 2D).

Precise positioning of the CCA-ends of A- and P-site tRNAs at the PTC is necessary to ensure efficient peptide-bond formation (Fig. 3A). Specific conformational changes of highly conserved nucleotides of the 23S rRNA within the PTC are associated with binding of different ligands to the PTC. For example, A2602 and U2585 adopt dramatically different conformations in ribosome structures in various functional states (Fig. 3B) (21). In the PTC of the 70S•TnaC complex, clear density for A2602 indicates that this nucleotide adopts a distinct conformation (Fig. 3C), in contrast to the RNC-70S complex where it appears to be disordered (Fig. 3D). In the 70S•TnaC map, visualization of a single nucleotide is also exemplified by A1493 in the decoding center of the 30S (Fig. S9). The A2602 conformation resembles that of the PTC when the translation inhibitor sparsomycin is bound (Fig. 3E) (22). In addition to A2602, continuous density between the nascent chain and the location of U2585, suggests that this flexible base (see Fig. 3B) shifts to interact with Pro^{24} of TnaC (Fig. 3C). Inactivation of the PTC in the 70S•TnaC complex requires free tryptophan, whose binding site has been proposed to overlap with that of the antibiotic sparsomycin (12,20,23) and with the amino-acyl moiety of an A-tRNA at the PTC (10). Nevertheless, no additional density could be attributed to a free tryptophan molecule (Fig. 3E), despite the purification and cryo-EM analysis in the presence of 2 mM tryptophan (14). The conformations of A2602 and U2585 observed in the 70S•TnaC complex are incompatible with simultaneous cohabitation of termination release factors (RFs) (Fig. 3F) (24). Thus, even if RFs can still bind to the stalled 70S•TnaC complexes (11), the fixed conformation of A2602 and U2585 would prevent correct positioning of the GGQ motif of the RF within the PTC that is necessary for efficient hydrolysis and release of the nascent chain from the P-tRNA (24).

Since residues of the nascent chain that are essential for TnaC-mediated stalling are located far from the PTC, a signal must be propagated from the depths of the tunnel back to the PTC (Fig. 4). Our map allows us to rule out the idea that peptide stalling initiates a cascade of large-scale conformational changes throughout the ribosome, ultimately leading to the inhibition of translation (25). Consequently, the "stalling signal" may be relayed back through the nascent chain itself, i.e. the interaction between the nascent chain and the tunnel induces a specific conformation in the nascent chain that feedback inhibits the PTC (Relay R1 in Fig. 4B), and/or through a series of subtle conformational changes in the network of ribosomal components that comprise the tunnel (R2 and R3 in Fig. 4B).

The surface of the exit tunnel has been described as being "Teflon-like" due to its predominantly hydrophilic nature (26). Yet here we have shown that the TnaC-stalled nascent

chain makes extensive interactions with the ribosome along the entire length of the exit tunnel (Fig. 4C and Fig. S6). This is important to emphasize since density is visible for ~10 of the amino acids preceding the canonical TnaC sequence, indicating that even residues unrelated to the stalling process can adopt a distinct conformation within the exit tunnel. This notion is supported by a cryo-EM structure of a yeast 80S ribosome-nascent chain complex stalled during the translation of a truncated dipeptidyl-aminopeptidase B (DP120) mRNA at 6.1 Å resolution (27). Although the DP120 sequence has no stalling capacity, density for this nascent chain is visible, indicating a preferred conformation within the exit tunnel (Fig. 4D). Notably, the DP120 nascent chain follows a different path from that reported here for TnaC (Fig. 4E, F). Clearly the chemical and electrostatic properties of the tunnel environment play a pivotal role in facilitating this kind of distinct nascent chain behavior (3,4). The finding that nascent chains with little or no sequence conservation interact with the exit tunnel in a distinct manner and adopt individual conformations may be important not only for initial folding events (1-3), but also for the variety of nascent chain-mediated regulatory mechanisms (5).

Supplementary Material

Refer to Web version on PubMed Central for supplementary material.

Acknowledgments

This research was supported by grants from the Deutsche Forschungsgemeinschaft SFB594 and SFB646 (to R.B.), SFB740 (to T.M.) and WI3285/1-1 (to D.N.W.), by NIH grants GM022778 (to T.A.S.) and P41-RR05969 (to K.S.), by NSF grant PHY0822613 (to K.S.), by the European Union and Senatsverwaltung für Wissenschaft, Forschung und Kultur Berlin (UltraStructureNetwork, Anwenderzentrum). Computer time for MDFF was provided through an NSF Large Resources Allocation Committee grant MCA93S028. Coordinates of the atomic models of TnaC-70S complex have been deposited in the PDB under accession numbers 3xxx and 3xxx. The cryo-electron microscopic map has been deposited in the 3D-EM database under accession number EMDxxxx.

References and Notes

1. Woolhead CA, McCormick PJ, Johnson AE. Cell 2004;116:725–36. [PubMed: 15006354]
2. Lu J, Deutsch C. Biochemistry 2005;44:8230–43. [PubMed: 15938612]
3. Lu J, Deutsch C. Nat Struct Mol Biol 2005;12:1123–9. [PubMed: 16299515]
4. Lu J, Deutsch C. J Mol Biol 2008;384:73–86. [PubMed: 18822297]
5. Tenson T, Ehrenberg M. Cell 2002;108:591–4. [PubMed: 11893330]
6. Nakatogawa H, Ito K. Cell 2002;108:629–36. [PubMed: 11893334]
7. Woolhead CA, Johnson AE, Bernstein HD. Mol Cell 2006;22:587–98. [PubMed: 16762832]
8. Yap MN, Bernstein HD. Mol Cell 2009;34:201–11. [PubMed: 19394297]
9. Oliver D, Norman J, Sarker S. J Bacteriol 1998;180:5240–2. [PubMed: 9748461]
10. Gong F, C Y. Science 2002;297:1864–7. [PubMed: 12228716]
11. Cruz-Vera L, Rajagopal S, Squires C, Yanofsky C. Mol Cell 2005;19:333–43. [PubMed: 16061180]
12. Cruz-Vera LR, Yanofsky C. J Bacteriol 2008;190:4791–7. [PubMed: 18424524]
13. Gong F, Ito K, Nakamura Y, Yanofsky C. Proc Natl Acad Sci USA 2001;98:8997–9001. [PubMed: 11470925]
14. see Supporting Online Material.
15. Trabuco LG, Villa E, Mitra K, Frank J, Schulten K. Structure 2008;16:673–83. [PubMed: 18462672]
16. de Bakker PI, Furnham N, Blundell TL, DePristo MA. Curr Opin Struct Biol 2006;16:160–5. [PubMed: 16483766]
17. Simonovic M, Steitz TA. Biochim Biophys Acta. 2009
18. Yang R, Cruz-Vera LR, Yanofsky C. J Bacteriol 2009;191:3445–50. [PubMed: 19329641]
19. Vazquez-Laslop N, Thum C, Mankin AS. Mol Cell 2008;30:190–202. [PubMed: 18439898]
20. Cruz-Vera LR, New A, Squires C, Yanofsky C. J Bacteriol 2007;189:3140–6. [PubMed: 17293420]

21. Schmeing TM, Huang KS, Strobel SA, Steitz TA. Nature 2005;438:520–4. [PubMed: 16306996]
22. Schmeing TM, Huang KS, Kitchen DE, Strobel SA, Steitz TA. Mol Cell 2005;20:437–48. [PubMed: 16285925]
23. Cruz-Vera LR, Gong M, Yanofsky C. Proc Natl Acad Sci USA 2006;103:3598–603. [PubMed: 16505360]
24. Weixlbaumer A, et al. Science 2008;322:953–6. [PubMed: 18988853]
25. Mitra K, et al. Mol Cell 2006;22:533–43. [PubMed: 16713583]
26. Nissen P, Hansen J, Ban N, Moore PB, Steitz TA. Science 2000;289:920–30. [PubMed: 10937990]
27. Becker T, et al. Science 2009;X:xxx–xxx.

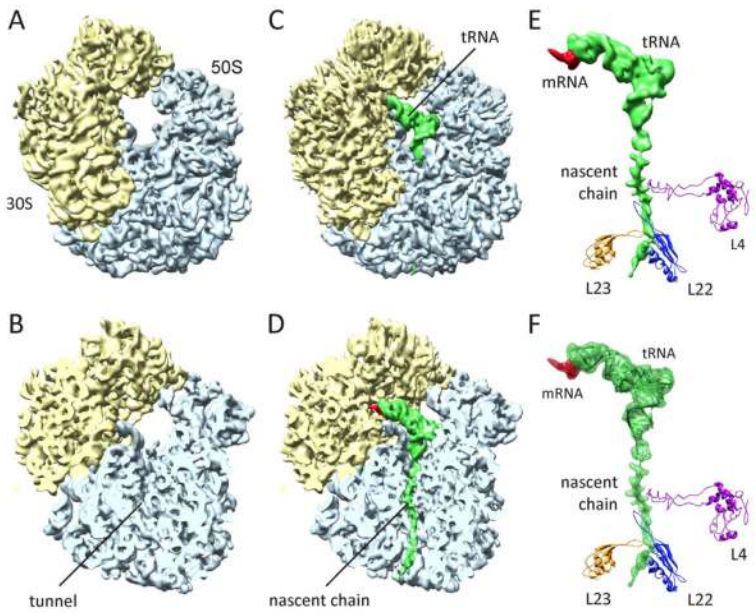

Fig. 1.

Cryo-EM reconstruction of the TnaC•70S complex. (**A-B**) Cryo-EM reconstruction of the control *E. coli* 70S ribosome at 6.6 Å resolution, with small and large subunit colored yellow and blue, respectively. (**C-D**) The 5.8 Å resolution cryo-EM density of the TnaC•70S complex, with density for the TnaC-tRNA shown in green. (**E**) Isolated density for the TnaCtRNA (green) and mRNA (red) from (C). The relative positions of ribosomal proteins L4 (purple), L22 (blue) and L23 (yellow) are indicated. (**F**) Fitting of molecular models for the TnaC-$tRNA^{Pro}$ into the cryo-EM density from (E).

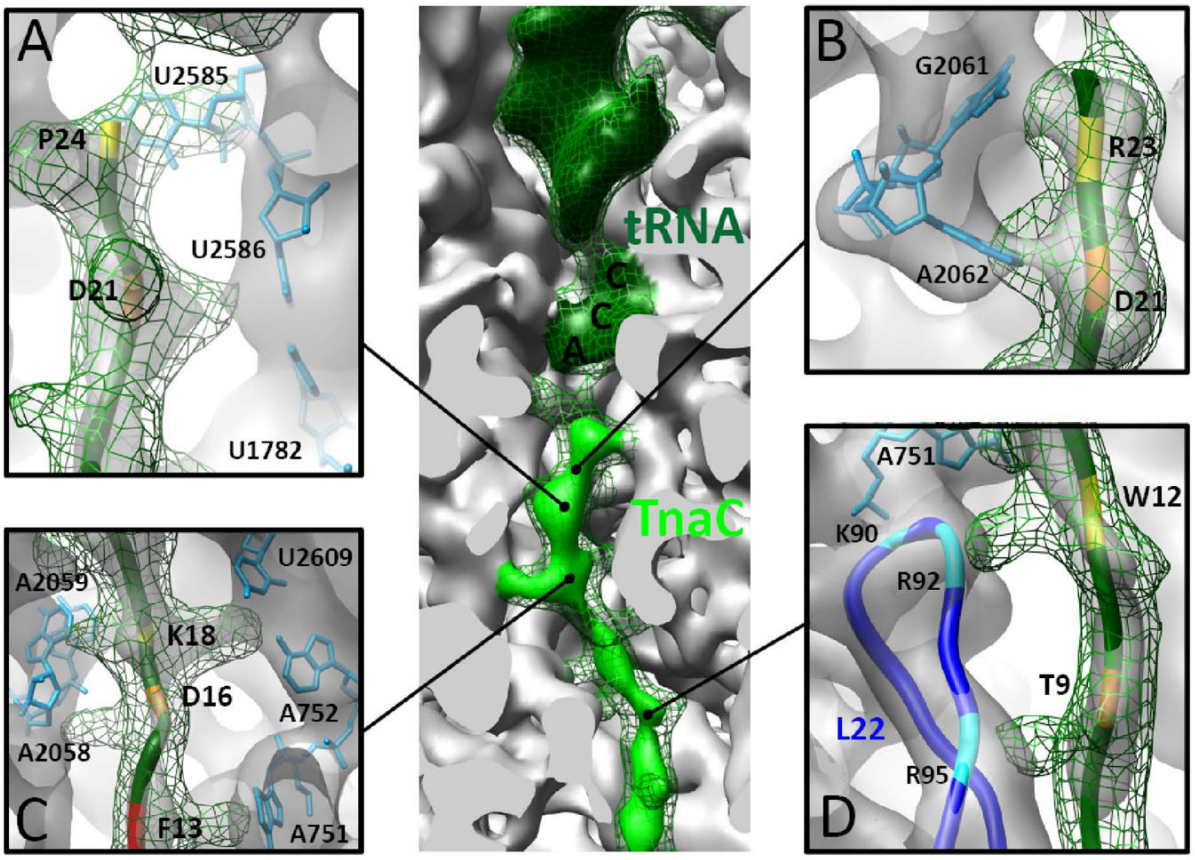

Fig. 2.

Interaction between the TnaC nascent chain and the ribosomal tunnel. The central panel shows a section through the large subunit revealing contact points between the TnaC nascent chain (light green) and the ribosome (gray). Density attributed to the P-tRNA is coloured dark green, and for peptidyl-tRNA at a lower threshold is shown as a green mesh. (**A**)-(**D**) Different views of connections between the nascent chain (green ribbon) and the 23S rRNA (blue sticks) or ribosomal protein L22 (blue ribbon). Density for the TnaC•70S complex is shown as a transparent gray surface, whereas the isolated nascent chain at a lower threshold is shown as a green mesh. Important TnaC residues are highlighted yellow, orange or red.

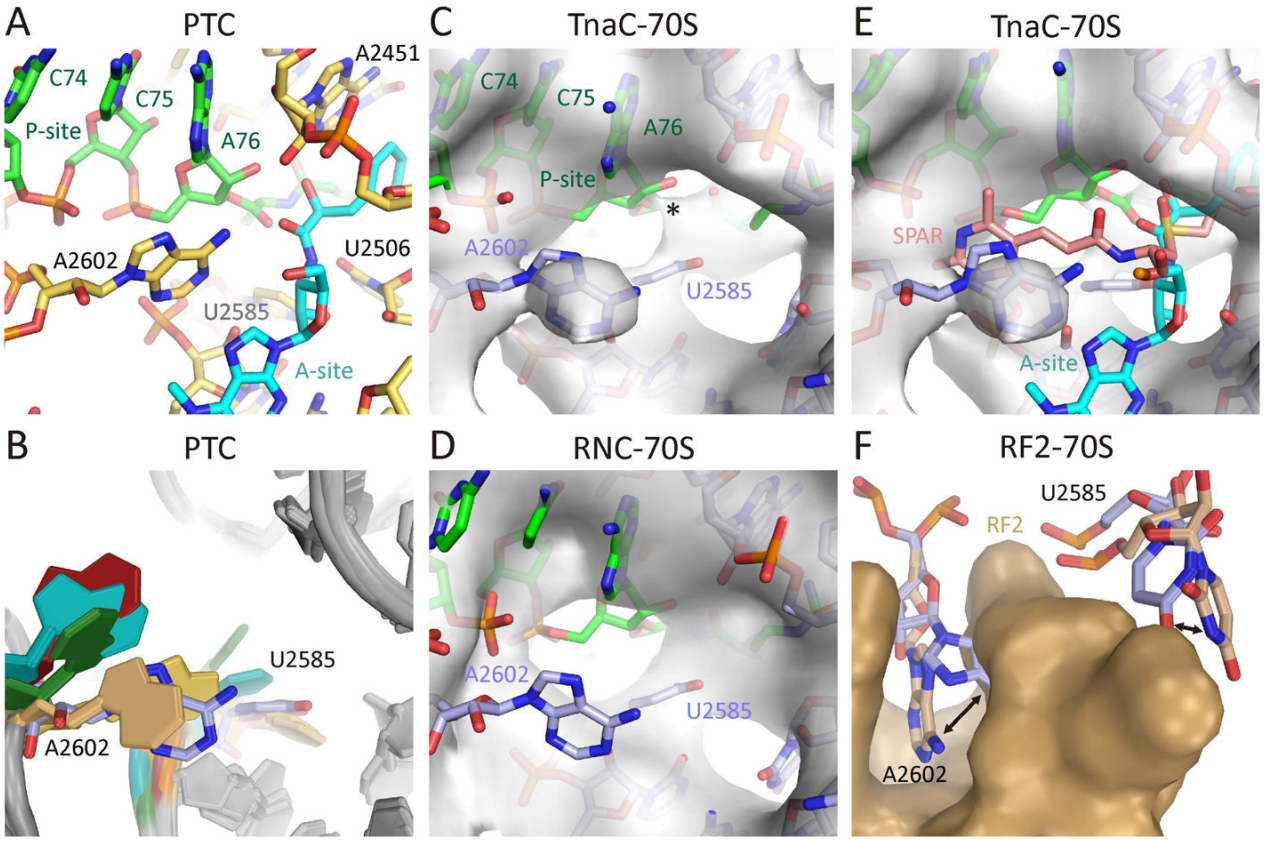

Fig. 3.

Silencing of the peptidyltransferase center (PTC). (**A**) Conformation of 23S rRNA nucleotides at the PTC when tRNA CCA-end mimics are bound to A- (cyan) and P-sites (green) (PDB1VQN). (**B**) Comparison of A2602 and U2585 conformations in various ribosome crystal structures (red, PDB1VQK; teal, PDB1S72; yellow, PDB2I2T; gold, PDB2JL5/6; blue, PDB1VQ9; green, PDB1VQN). (**C**) View into the PTC of the TnaC-70S complex, with the MDFF model of the TnaC-tRNA (green) and nucleotides of the 23S rRNA (blue). The cryo-EM density is shown as a transparent gray surface, with an asterisk indicating the connection between P-tRNA and nascent chain. (**D**) View into the PTC of 70SRNC complex, with fitted models as in (A). Note the lack of density (gray) for nucleotide A2602. (**E**) As in (A), but with the antibiotic sparsomycin (SPAR, red; PDB1VQ9) and the terminal A76 and aminoacyl moiety of an A-tRNA (cyan; PDB1VQN) included. (**F**) Comparison of A2602 and U2585 positions (arrowed) between TnaC-70S complex (blue) and RF2-70S complex (24); gold), with RF2 shown as surface representation (gold).

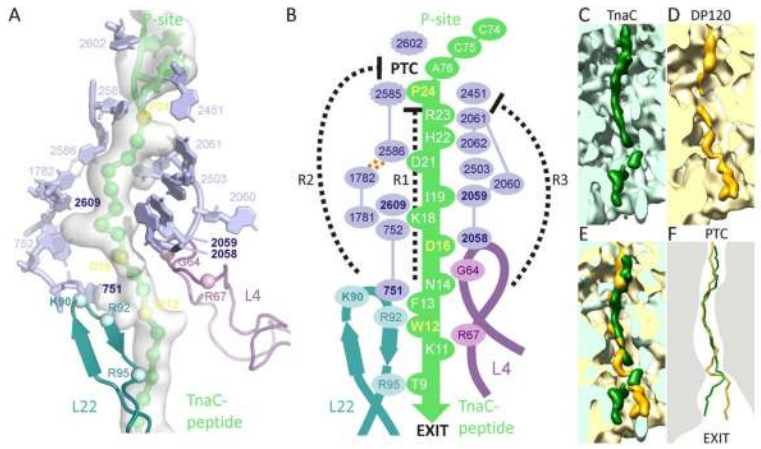

Fig. 4.

Relay for PTC silencing and the path of the nascent chain. (**A**) Ribosomal components potentially involved in a relay mechanism to inactivate the PTC, with those implicated in stalling in bold. The TnaC nascent chain is in green, with residues essential for stalling colored yellow. The isolated TnaC-tRNA density is shown as a transparent gray surface. (**B**) Schematic indicating potential relay pathways from Trp^{12} (W12) of TnaC to the PTC, either through the nascent chain itself (R1) or via networks of interconnected 23S rRNA nucleotides (R2 and R3). (**C-D**) Transverse section through the large subunit showing the path of (**C**) TnaC (dark green) and (**D**) DP120 (35); orange) nascent chains through the ribosomal tunnel. (**E**) Superposition of (A) and (B). (**F**) Schematic highlighting the similarities and differences between the TnaC and DP120 nascent chain in terms of contacts and passage through the tunnel.